

# COMPUTER MODELING AND SIMULATION OF HUMAN MOVEMENT

---

Marcus G. Pandy

*Department of Kinesiology and Department of Biomedical Engineering, University of  
Texas at Austin, Austin, Texas 78712; e-mail: pandy@mail.utexas.edu*

**Key Words** musculoskeletal, joint, muscle coordination, walking, jumping,  
pedaling

■ **Abstract** Recent interest in using modeling and simulation to study movement is driven by the belief that this approach can provide insight into how the nervous system and muscles interact to produce coordinated motion of the body parts. With the computational resources available today, large-scale models of the body can be used to produce realistic simulations of movement that are an order of magnitude more complex than those produced just 10 years ago. This chapter reviews how the structure of the neuromusculoskeletal system is commonly represented in a multijoint model of movement, how modeling may be combined with optimization theory to simulate the dynamics of a motor task, and how model output can be analyzed to describe and explain muscle function. Some results obtained from simulations of jumping, pedaling, and walking are also reviewed to illustrate the approach.

## CONTENTS

INTRODUCTION .....	246
WHAT SHOULD A MODEL OF MOVEMENT INCLUDE? .....	246
Modeling Skeletal Dynamics .....	248
Modeling Muscle Paths .....	252
Modeling Musculotendon Actuation .....	253
Modeling Muscle Excitation-Contraction Coupling .....	254
Modeling the Goal of the Motor Task .....	255
DETERMINING MUSCLE FORCE: DYNAMIC OPTIMIZATION SOLUTIONS ARE PREDICTIVE .....	256
HIGH-PERFORMANCE COMPUTING AND VISUALIZATION CAN BE APPLIED TO PRODUCE REALISTIC SIMULATIONS OF MOVEMENT .....	258
Dynamic Optimization Problems can be Parameterized .....	258
Dynamic Optimization Problems can be Parallelized .....	260
Simulations of Movement Should be Visualized .....	260
HOW MODELING AND EXPERIMENTATION CAN BE INTEGRATED TO STUDY MOVEMENT .....	260

HOW SHOULD MODEL OUTPUT BE ANALYZED? ..... 262

MODEL SIMULATIONS CAN REVEAL FUNCTION ..... 263

    Jumping ..... 263

    Pedaling ..... 265

    Walking ..... 265

LOOKING AHEAD ..... 266

INTRODUCTION

One can learn a lot by doing experiments on people. In gait-analysis experiments, for example, high-speed camera systems are used to track the changing positions and orientations of the body segments, strain-gauge or piezoelectric transducers are used to measure the magnitudes and directions of the resultant forces exerted on the ground, and surface or in-dwelling electromyography (EMG) electrodes are used to record the sequence and timing of muscle activity (1–3). These data provide a quantitative description of the kinematics and dynamics of body-segmental movement, but they do not explain how muscles work together to produce a coordinated gait pattern; specifically, kinematic, ground-reaction force, and muscle EMG data alone do not explain how each muscle accelerates each and every body segment at each instant during the gait cycle.

Computer modeling and simulation has risen to new heights in recent years, mainly because of the growing belief that this approach can provide more quantitative explanations of how the neuromuscular and musculoskeletal systems interact to produce movement. Simulations of standing, walking, jumping, and pedaling, in particular, have provided considerable insight into how the leg muscles work together to achieve a common goal during each of these tasks (4–10). Interest in using models to study movement has been, and continues to be, fueled also by the ever-increasing performance of computers. With the computational resources available today, large-scale models of the body [i.e. models that have many degrees of freedom (dof) and are actuated by many muscles] may be used to perform realistic simulations of movement that are an order of magnitude more complex than those performed just 10 years ago. In this chapter I review how the structures of the neuromuscular and musculoskeletal systems may be represented in a mathematical (computer) model of the body, how these elements may be integrated to simulate the dynamics of a motor task, and how model output can be analyzed to describe and explain muscle function during multijoint movement.

WHAT SHOULD A MODEL OF MOVEMENT INCLUDE?

What to include in a model of movement depends on the intended use of the model. If the overall goal is to understand muscle coordination, a model that does not include joints and muscles is not likely to be useful. For example, the simplest model used to study walking is the inverted pendulum (11–13) (Figure 1*a*). This

Annu. Rev. Biomed. Eng. 2001.3:245-273. Downloaded from arjournals.annualreviews.org by b-on: Universidade Nova de Lisboa (UNL) on 02/08/07. For personal use only.

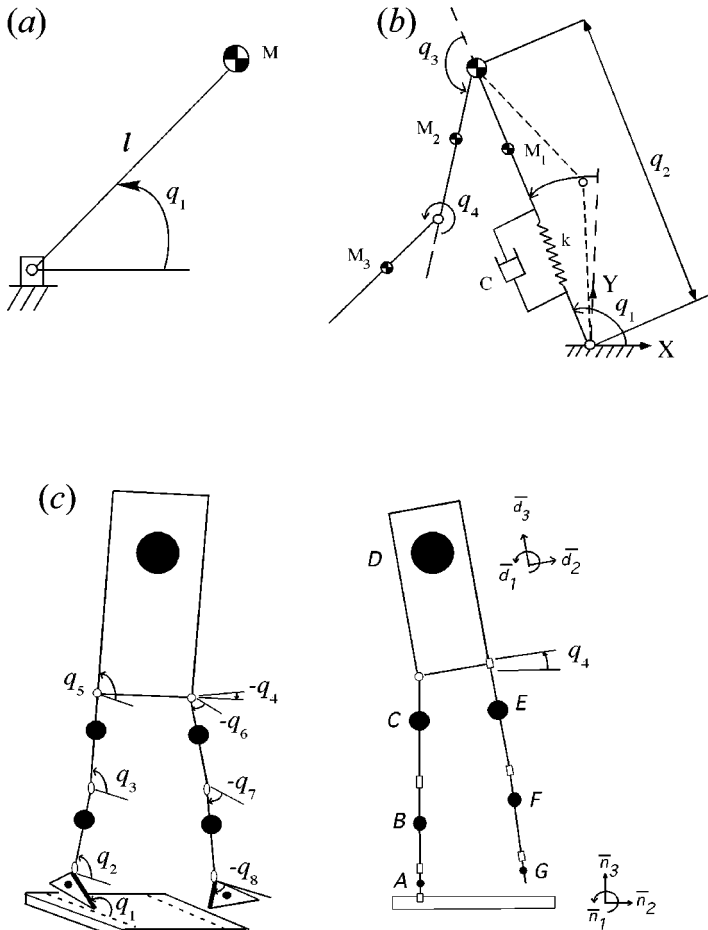


**Figure 1** Increasing complexity of models used to simulate normal walking on level ground. (a) Planar 1 degree-of-freedom (dof) pendulum model used to simulate the single support phase (11, 13). (b) Planar 3-dof model used to simulate the single support phase (16). (c) Three-dimensional, 8-dof model of the body used to simulate the full-gait cycle, except the period near toe-off (4).

model can describe the efficient transfer of kinetic and potential energy that takes place when people walk at freely selected cadences and step lengths (11, 13), but it cannot teach us much about how the leg muscles cooperate to produce a smooth pathway of the body's center of mass. Models with joints but no muscles (i.e. those actuated by joint torques instead of muscle forces) are also not likely to be useful in coordination studies because these models represent only the net effect of the muscles around each joint (14–17). Indeed, torque-actuated models can sometimes

lead to incorrect interpretations of muscle function, as has been demonstrated in pedaling, for example (8, 9).

For good reason, structures contributing to the overall stiffness of a joint (i.e. cartilage, menisci, ligaments, and capsule) are usually not included in multijoint models used to study movement. This level of detail does not seem warranted, especially if the goal is to explain muscle function. If ligament action is represented at all, it is usually in the form of a passive joint torque, with the magnitude of the torque increasing exponentially near the limits of the joint's range of motion (18–23). Cartilage and the menisci are rarely, if ever, included, the reason being that these structures do not alter the forces transmitted by the joint; cartilage and the menisci serve instead to decrease the joint contact stresses by increasing the contact areas between the bones (24).

Movement simulations ought to include (a) a model of the skeleton, (b) a model of the muscle paths, (c) a model of musculotendon actuation, (d) a model of muscle excitation-contraction coupling, and (e) a model of the goal of the motor task (see Figure 2).

## Modeling Skeletal Dynamics

Most simulations of multijoint movement are planar; for example, sagittal-plane models of the body have been used to simulate standing, walking, running, jumping, and pedaling (5, 8–10, 25–32). The rationale is fairly simple. Firstly, flexion and extension represent the major movements at most joints, so they contribute most significantly to performance in most tasks (e.g. the vertical position of the body's center of mass during the ground-contact phase of jumping is determined almost entirely by flexion and extension of the hip, knee, and ankle) (5, 30–33). Furthermore, planar models with hinge joints have fewer dofs than do three-dimensional models with, say, hinge, universal, and ball-and-socket joints; therefore, simulations based on planar models generally take less computer time than do those that allow movement of the body parts in three dimensions.

Whether a motor task should be simulated in two or three dimensions depends mainly on the question being asked. For example, a planar model is most probably adequate for studying the contribution of stance knee flexion-extension to motion of the center of mass during normal gait (14, 16) (Figure 1b). However, this model cannot be used to determine the relative contributions of stance knee flexion-extension, pelvic list, and pelvic rotation because the latter two movements occur mainly in the frontal and transverse planes, respectively (34). The model shown in Figure 1c can be used to study the contributions of stance knee flexion-extension

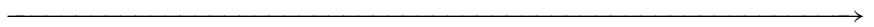


**Figure 2** Diagram showing the components most commonly included in a multijoint model of movement. The *insets* show specific models of muscle excitation-contraction coupling, musculotendon actuation, muscle-path geometry, and the skeletons that were used to simulate jumping and walking (23, 38, 71).



and pelvic list, but not that of pelvic rotation, because this movement is not represented explicitly here. Figure 3*a* shows a three-dimensional, 10-segment, 23-dof model of the skeleton, which has been used to simulate one cycle of normal walking (23). Because it embodies all six major determinants of gait (i.e. hip, knee, and ankle flexion-extension, pelvic rotation, pelvic list, and lateral pelvic displacement) (34), this model may be used to study the effects of hip, knee, and ankle flexion-extension versus movements of the pelvis in the transverse and frontal planes.

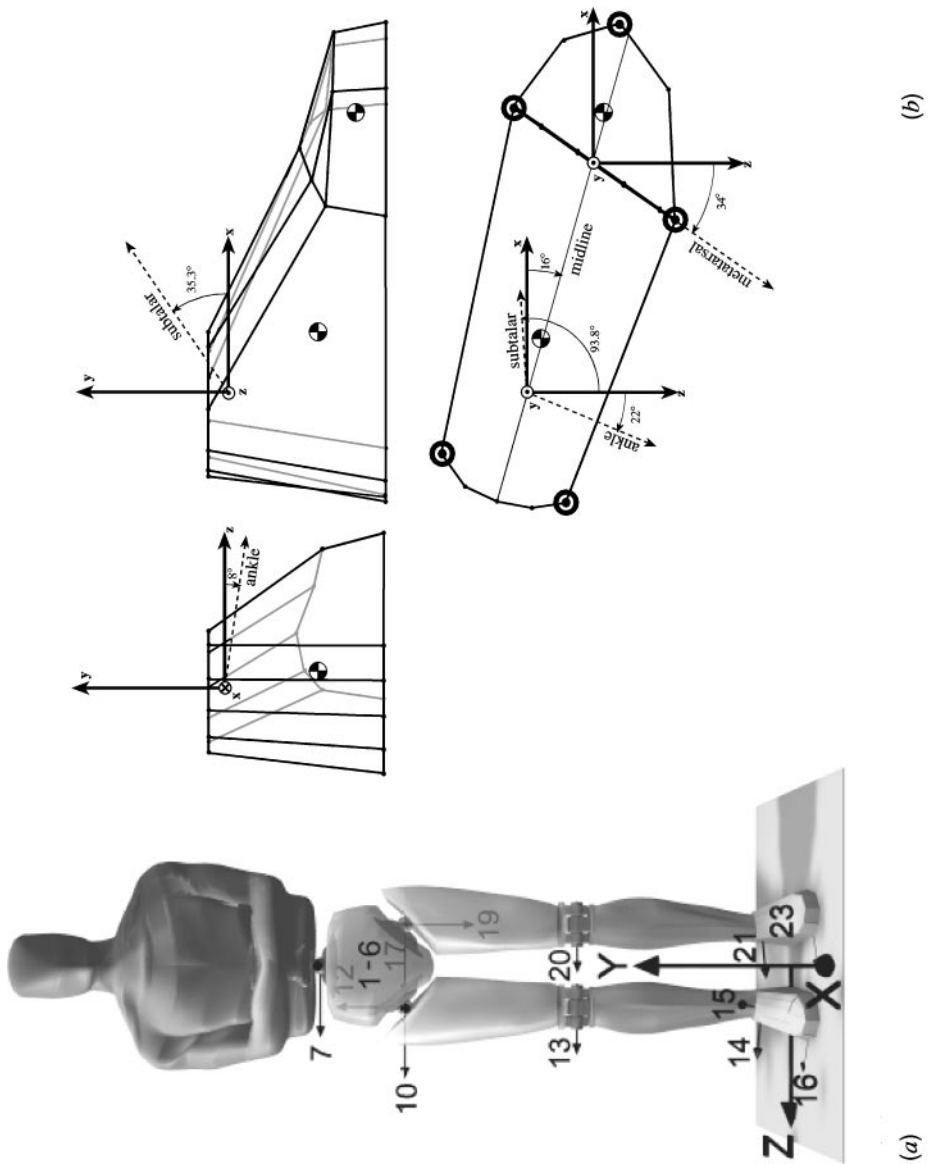
Regardless of whether the skeleton is modeled in two or three dimensions, the relationships between the forces applied to the body and the resulting motion of the body segments can always be expressed in the form

$$M(\underline{q})\ddot{\underline{q}} + C(\underline{q})\dot{\underline{q}}^2 + \underline{G}(\underline{q}) + R(\underline{q})\underline{F}^{MT} + \underline{E}(\underline{q}, \dot{\underline{q}}) = \underline{0}, \quad (1)$$

where  $\underline{q}$ ,  $\dot{\underline{q}}$ ,  $\ddot{\underline{q}}$  are vectors of the generalized coordinates, velocities, and accelerations, respectively;  $M(\underline{q})$  is the system mass matrix and  $M(\underline{q})\ddot{\underline{q}}$  a vector of inertial forces and torques;  $C(\underline{q})\dot{\underline{q}}^2$  is a vector of centrifugal and Coriolis forces and torques;  $\underline{G}(\underline{q})$  is a vector of gravitational forces and torques;  $R(\underline{q})$  is the matrix of muscle moment arms;  $\underline{F}^{MT}$  is a vector of musculotendon forces and  $R(\underline{q})\underline{F}^{MT}$  a vector of musculotendon torques; and  $\underline{E}(\underline{q}, \dot{\underline{q}})$  is a vector of external forces and torques applied to the body by the environment.

One of the more difficult parts of developing a model of skeletal dynamics is dealing with contact between the body and the environment. Practically

**Figure 3** (a) Ten-segment, 23-dof model of the skeleton used to simulate normal walking (23, 71). The model skeleton was actuated by 54 muscles (not shown). Six generalized coordinates were used to reproduce all possible movements of the pelvis in space; the remaining nine segments branch in an open chain from the pelvis. The head, arms, and torso, represented as a single rigid body, articulates with the pelvis via a 3-dof ball-and-socket joint located at the third lumbar vertebra. Each hip was modeled as a 3-dof ball-and-socket joint, each knee as a 1-dof hinge joint, each ankle as a 2-dof universal joint, and each metatarsal joint as a 1-dof hinge. Each foot was modeled using two segments, a hindfoot, and a toes segment (see *b*). Because the pelvis has 6 dof, each foot is free to make and break contact with the ground. (b) Diagram showing the right foot of the model shown in *a*. The ankle and subtalar axes are projected onto the frontal plane (*top left*), sagittal plane (*top right*), and transverse plane (*bottom*). The metatarsal axis is shown in the transverse plane and lies at the sole of the foot (*bottom*, metatarsal). The *x*, *y*, and *z* axes define the fore-aft, vertical, and transverse directions, respectively. The vertices and connecting lines represent the volume of a foot plus a size-10 tennis shoe. The *circled dots* drawn in the transverse plane (*bottom*) show the locations of five ground springs placed under the foot. These springs were used to simulate the interaction of the foot with the ground during walking. (Modified from Reference 38.)



all simulations of movement treat this interaction in a simple way. For example, simulations of walking often ignore the changes in velocity and acceleration that occur at heel contact by modeling the single and double support phases separately (26, 35, 36). Figure 3*b* illustrates an alternate approach in which the compliance between the body and the ground is modeled using a series of damped springs (4, 23, 29, 37). Each ground spring is three dimensional, meaning it applies a force simultaneously in the vertical, fore-aft, and transverse directions. The interaction between the foot and the ground can be simulated very efficiently with this model because the vertical force applied by each spring varies exponentially with the height of the foot above the ground (for details, see 38).

If the number of dofs of the model skeleton is greater than, say, four, then a computer is needed to obtain Equation 1 explicitly. A number of commercial software packages are available for this purpose, including AUTOLEV by On-Line Dynamics Inc, SD/FAST by Symbolic Dynamics Inc, ADAMS by Mechanical Dynamics Inc, and DADS by CADSI.

## Modeling Muscle Paths

All multijoint models of movement assume that the muscle tendons insert at single points on the bones (4, 5, 9, 10, 23, 39–46). When a muscle inserts over a large area of bone, it is usually separated into two or more portions, as illustrated in Figure 4.

Two different methods are commonly used to model the paths of muscles in the body: the straight-line and centroid-line methods. In the straight-line method, the path of a muscle is represented by a straight line joining the centroids of the muscle attachment sites (46–49). Although this method is easy to implement, when a muscle wraps around a bone or another muscle, it may not produce meaningful results (Figure 5). In the centroid-line method, the muscle path is represented as a line passing through the locus of cross-sectional centroids of the muscle (47). Although the muscle's line of action is represented more accurately in this way, the centroid-line method can be difficult to apply because (*a*) it may not be possible to obtain the locations of the muscle cross-sectional centroids for even a single position of the body, and (*b*) even if a muscle's centroid path is known for one position of the body, it is practically impossible to determine how the muscle's path changes as body position changes (47).

One way of addressing this problem is to introduce effective attachment sites or via points at specific locations along the centroid path. In this approach, the muscle's line of action is defined by using either straight-line segments or a combination of straight-line and curved-line segments between each set of via points (50, 51). The via points remain fixed relative to the bones even as the joints move, and muscle wrapping is taken into account by making the via points active or inactive, depending on the configuration of the joint. This method works without any difficulties when a muscle spans a 1-dof hinge joint, but it can lead to discontinuities in the calculated values of moment arms when joints have more



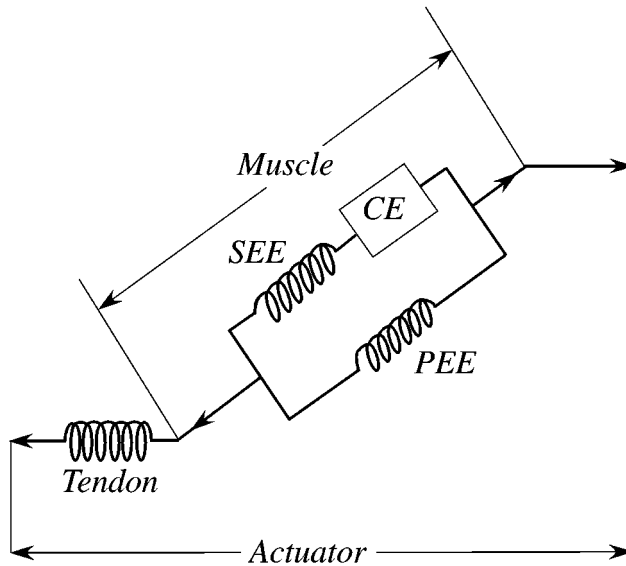


**Figure 6** Schematic diagram of a model commonly used to simulate musculotendon actuation. Each musculotendon actuator is represented as a 3-element muscle in series with an elastic tendon. The mechanical behavior of muscle is described by a Hill-type contractile element (CE) that models muscle's force-length-velocity property, a series-elastic element (SEE) that models muscle's active stiffness, and a parallel-elastic element (PEE) that models muscle's passive stiffness. The instantaneous length of the actuator is determined by the length of the muscle, the length of the tendon, and the pennation angle of the muscle. In this model, the width of the muscle is assumed to remain constant as muscle length changes. (Modified from References 5, 57.)

than 1 rotational dof. An alternate approach, called the obstacle-set method, eliminates this problem by allowing the muscle to slide freely over the bones and other muscles as the configuration of the joint changes (52–55). Because the path of a muscle is not constrained by contact with the neighboring muscles and bones, the obstacle-set method produces smooth moment arm-joint angle curves (Figure 5b).

## Modeling Musculotendon Actuation

When muscles are included in a model of movement, their mechanical behavior is often described by a three-element, Hill-type model (56, 57). In the model shown in Figure 6, muscle's force-producing properties are described by four parameters: a muscle's peak isometric force ( $F_o^m$ ) and corresponding fiber length ( $l_o^m$ ) and pennation angle ( $\alpha$ ), and the intrinsic shortening velocity of muscle ( $v_{\max}$ ).  $F_o^m$  is usually obtained by multiplying muscle's physiological cross-sectional area by a

generic value of specific tension (46, 51, 57). Values of  $l_o^m$  (the length at which active muscle force peaks) and  $\alpha$  (the angle at which muscle fibers insert on tendon when the fibers are at their optimal length) are almost always based on data obtained from cadaver dissections (58, 59).  $v_{\max}$  is assumed to be muscle-independent in most simulations of movement. For example, simulations of jumping (5, 23, 30), pedaling (9, 10), and walking (23) assume  $v_{\max} = 10 \text{ s}^{-1}$  for all muscles, which models the summed effect of slow, intermediate, and fast fibers (57). Very few studies have examined the sensitivity of model simulations to changes in  $v_{\max}$ , even though a change in the value of this parameter affects performance nearly as much as a change in the value of  $F_o^m$  (60).

Tendon is usually represented as an elastic element (5, 9, 23, 46, 51, 57). Even though force varies nonlinearly with a change in length as tendon is stretched from its rest length,  $l_s^T$  (61, 62), a linear force-length curve is sometimes used (5, 30, 38, 60). This simplification will overestimate the amount of strain energy stored in tendon, but the effect on actuator performance is not likely to be significant because tendon force is small in the region where the force-length curve is nonlinear. However, actuator performance does depend strongly on the value assumed for  $l_s^T$ , which is important because this parameter is difficult to measure. Changing the value of  $l_s^T$  in the model of Figure 6 can change not only the magnitude of the peak force developed by the actuator, but also the joint angle at which peak force occurs (46, 51, 57). Thus, the value of  $l_s^T$  and, more specifically, the value of the ratio of optimal muscle-fiber length to tendon rest length,  $l_o^m / l_s^T$ , assumed in the model can significantly affect predictions of muscle coordination.

For the actuator shown in Figure 6, musculotendon dynamics is described by a single, nonlinear, differential equation that relates musculotendon force ( $F^{MT}$ ), musculotendon length ( $l^{MT}$ ), musculotendon shortening velocity ( $v^{MT}$ ), and muscle activation ( $a^m$ ) to the time rate of change in musculotendon force:

$$\dot{F}^{MT} = f(F^{MT}, l^{MT}, v^{MT}, a_m); 0 \leq a_m \leq 1. \quad (2)$$

Given values of  $F^{MT}$ ,  $l^{MT}$ ,  $v^{MT}$ , and  $a^m$  at one instant in time, Equation 2 can be integrated numerically to find musculotendon force at the next instant.

## Modeling Muscle Excitation-Contraction Coupling

Muscle cannot be activated or relaxed instantaneously. The delay between muscle excitation and activation (or the development of muscle force) is due mainly to the time taken for calcium pumped out of the sarcoplasmic reticulum to travel down the T-tubule system and bind to troponin (63). The delay between muscle excitation ( $u$ , which represents the net neural drive) and muscle activation ( $a^m$ ) is usually modeled as a first-order process (5, 9, 10, 23, 28, 56, 57, 64):

$$\dot{a}^m = (1/\tau_{\text{rise}})(u^2 - ua^m) + 1/\tau_{\text{fall}}(u - a^m); u = u(t); a^m = a^m(t). \quad (3)$$

Other forms of this relation are also possible; for example, an equation that is linear in the control,  $u$ , has been used to simulate jumping (5) as well as pedaling (9).

Implicit in the formulation of Equation 3 is the assumption that muscle activation depends only on a single variable  $u$ . Other models assume that  $a$  depends on two inputs,  $u_1$  and  $u_2$ , say, which represent the separate effects of recruitment and stimulation frequency (65, 66). In simulations of multijoint movement, whether both recruitment and stimulation frequency are incorporated in a model of excitation-contraction coupling is probably not as important as the values assumed for the time constants,  $\tau_{\text{rise}}$  and  $\tau_{\text{fall}}$ . Values of these constants range from 12–20 ms for rise time,  $\tau_{\text{rise}}$ , and from 24–200 ms for relaxation time,  $\tau_{\text{fall}}$  (5, 9, 28, 32, 57). Changes in the values of these constants within the ranges indicated can also have a significant effect on predictions of movement coordination (FC Anderson & MG Pandy, unpublished results).

## Modeling the Goal of the Motor Task

Equations 1–3 can be combined to form a model of the neuromusculoskeletal system. The inputs to this system are the muscle excitations, and the outputs are the body motions (Figure 2). Measurements of muscle EMG and body motions can be used to estimate muscle forces during movement (68, 69). Alternatively, the goal of the motor task can be modeled and used together with dynamic optimization theory to calculate the set of muscle excitations needed for optimal performance (see below). This approach has been used to simulate posture (25), standing up from a chair (70), walking (4, 23, 28, 71), jumping (5, 30–32, 38), and pedaling (8–10, 64).

Modeling the goal or cost function is not an easy proposition because performance is determined by the physiological and environmental constraints imposed on the task, and these factors can be difficult to quantify and describe mathematically. Take walking for example. It is difficult to know what, if any, criterion is used to produce the pattern of muscle activations and body-segmental motions that is observed when people walk at freely selected cadences and step lengths (44, 72, 73). For tasks such as walking, then, some measure of performance can be hypothesized, and once a simulation has been obtained, the model results can be compared with kinematic, external force, and muscle EMG measurements to support, reject, or refine the model of the goal (70, 74, 75). However, some tasks, such as minimum-time kicking (43), maximum-height jumping (5, 32, 38), maximum-speed pedaling (9), and maximum-distance throwing (76), present relatively unambiguous goals and are, therefore, well suited to the dynamic optimization approach. If the purpose of the task can be stated with a good deal of certainty (e.g. jump height is determined by the position and velocity of the body's center of mass at liftoff), the dynamic optimization approach can then be used to refine a model of the system dynamics. For example, the model of Figure 3 has been used to simulate both vertical jumping and walking (38, 71). Because the cost function for walking is ambiguous, the model was used first to solve a dynamic optimization problem for maximum-height jumping. Once the problem for jumping was solved and the response of the model validated against experimental data, the same model was

then used with greater confidence to simulate normal walking over level ground (38, 71, 77).

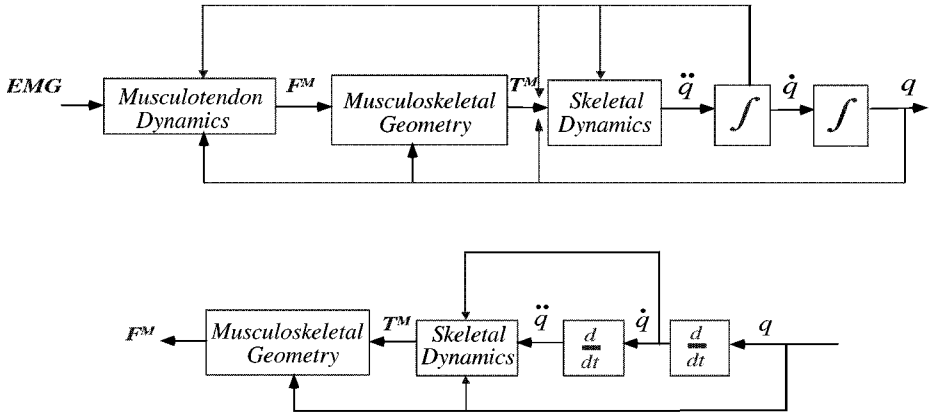
## DETERMINING MUSCLE FORCE: DYNAMIC OPTIMIZATION SOLUTIONS ARE PREDICTIVE

Once a model of the body has been formulated, it can be used to determine quantities that cannot be easily measured. For example, muscle forces cannot be measured noninvasively (78, 79), so these quantities are determined using either inverse or forward dynamics techniques. In the inverse dynamics method, noninvasive measurements of body motions (position, velocity, and acceleration of each segment) and external forces are used as inputs in Equation 1 to calculate muscle forces (41, 42, 44, 80). The forward dynamics method, on the other hand, uses muscle excitations (or muscle activations) as the inputs to calculate the corresponding body motions (Figure 7) (4–6, 9, 23, 28, 45, 64, 81). Because the number of muscles crossing a joint is greater than the number of dofs specifying joint movement, the force developed by each muscle cannot be determined uniquely. Virtually all attempts to solve this problem are based on the application of optimization theory (for a review, see 82; for variations on the optimization approach, see 27, 83–85).

Whereas the inverse dynamics (or static optimization) method solves a different optimization problem at each instant during the movement, the forward dynamics (or dynamic optimization) method solves one optimization problem for one complete cycle of the movement. This is the critical difference between these two methods, and it is also the reason dynamic optimization solutions are more expensive computationally (see below). Static optimization, on the other hand, has its own shortcomings. First, the validity of the results depends on the accuracy of the data recorded during a motion analysis experiment, specifically the positions, velocities, and accelerations of the body segments. The difficulty in accurately estimating velocity and acceleration from position measurements (86, 87) means that significant errors may be present in the calculated values of the net joint torques and, therefore, in the estimates of muscle force (41, 42, 45). Second, it is difficult to include muscle physiology in the formulation of a static optimization problem because estimates of muscle length and contraction velocity depend on the accuracy with which the positions and velocities of the body segments can be measured. Finally, static optimization is a descriptive or analysis-based approach: A model of the goal of the motor task cannot be included in the formulation of this problem. Dynamic optimization is more powerful because (a) the system equations (Equations 1–3) are integrated forward in time and, thus, muscle physiology is easily incorporated in the formulation of the problem, and (b) a model of the goal of the motor task can also be included because the optimization is done over a complete cycle of the task.

Do static and dynamic optimization solutions lead to the same results? The answer appears to be yes. For a comparison to be performed fairly, the same set of

### Forward Dynamics



### Inverse Dynamics

**Figure 7** Comparison of forward and inverse dynamics methods commonly used to determine muscle force. (Top) Muscle excitations are the inputs and body motions are the outputs in forward dynamics. Muscle force ( $F^M$ ) is an intermediate product (i.e. output of the model for musculotendon dynamics). If all the elements are modeled (i.e. skeletal dynamics, musculoskeletal geometry, and muscle actuation), and if the goal of the motor task is also modeled, then dynamic optimization can be applied to find the set of muscle excitations that produces an optimal performance. (Bottom) Body motions are the inputs and muscle forces are the outputs in inverse dynamics. Thus, measurements of body motions are used to calculate the net muscle torques exerted about the joints, from which muscle forces are determined using static optimization. EMG, electromyography. (Modified from Reference 82.)

body motions and joint torques must be used in both methods. This was done in a recent gait study, where the joint torques obtained from a dynamic optimization solution were used as the inputs to a set of analogous static optimization problems (88). Muscle physiology could be incorporated in the formulation of the static problems because the lengths and contraction velocities of the muscles were available from the dynamic solution. The static and dynamic solutions were found to be remarkably similar in their predictions of muscle force. Furthermore, muscle physiology had only a small effect on the character of the static solutions, indicating that the accuracy of the muscle forces derived from the static optimization method depends mainly on the values of the joint torques. Thus, static and dynamic optimization appear to give the same results, at least for relatively low-frequency movements like walking [however, Happee (66) shows that these two methods are also practically equivalent for higher-frequency, ballistic-type movements, such as throwing].

Which method should be used to determine muscle force? Provided accurate measurements of external forces and body motions are available, static optimization would be favored in calculations of muscle force, mainly because it is much less expensive computationally. If, however, the aim is to find how changes in body structure affect function and performance of a motor task, then dynamic optimization must be used because measurements of body motions and external forces are not available a priori in this instance (e.g. 60, 89, 90).

## HIGH-PERFORMANCE COMPUTING AND VISUALIZATION CAN BE APPLIED TO PRODUCE REALISTIC SIMULATIONS OF MOVEMENT

Early simulations of movement based on the application of dynamic optimization were limited mainly by the performance of the computers available at the time (43, 45, 91). With the computational power now available, large-scale models can be combined with dynamic optimization theory to produce simulations that are an order of magnitude more complex than those performed just 10 years ago. The feasibility of using dynamic optimization to produce realistic simulations of movement depends on three factors: (a) A robust computational algorithm is needed to converge to a solution of the dynamic optimization problem; (b) high-performance, parallel computers are needed to solve the problem in a reasonable amount of time; and (c) very fast computer graphics workstations are needed to visualize the simulation in real time (23, 38, 71, 92).

### Dynamic Optimization Problems can be Parameterized

Formulation of the dynamic optimization problem leads to a two-point, boundary-value problem (TPBVP), which can be solved by first integrating the system equations (Equations 1–3) forward in time and then integrating the adjoint or costate equations backward in time (93). Even when the number of dofs and the number of muscles represented in a model are small, fewer than 5, say, solution of the TPBVP can be difficult. The reason is that backward integration of the adjoint equations is unstable because of the high nonlinearity of these equations. Rather than solving the TPBVP directly, a better approach involves parameterizing the input control variables (e.g. muscle excitations) and converting the dynamic optimization problem into a parameter optimization problem (94). Given an initial guess for the values of the controls, the system equations are first integrated forward in time to evaluate the cost function and any constraints imposed on the simulated movement. Derivatives of the cost function and constraints are then calculated and used to find a new set of controls, which improves the values of the cost function and the constraints in the next iteration (see Figure 8). Although the parameter optimization algorithm shown in Figure 8 is more robust than any method used to solve the equivalent TPBVP (8–10, 94), this advantage must be weighed against

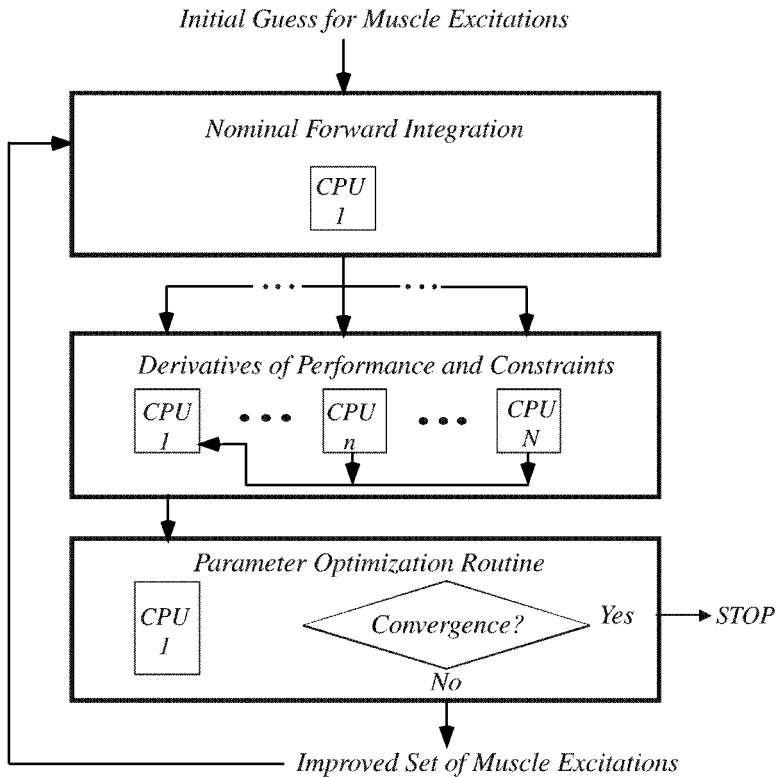


**Figure 8** Diagram illustrating the steps involved in solving a dynamic optimization problem using the method of parameter optimization. Each muscle excitation history or “control” is discretized into a set of independent variables. The problem is to calculate the values of the control variables that produce an optimal performance (e.g. maximize jump height). Linear interpolation is used to reconstruct the excitation history for each muscle once the values of the control variables have been found. Each iteration of the parameter optimization algorithm involves three steps: (a) Based on the initial guess for the controls, a forward integration of the system equations (Equations 1–3) is performed to evaluate the cost function and the constraints; (b) a series of forward integrations is then performed to evaluate the derivatives of the cost function and constraints with respect to each control variable; and (c) a parameter optimization routine is used to calculate a new set of control variables, one that improves the values of either the cost function or the constraints. A parallel computer can be used to calculate the derivatives of the cost function and the constraints with respect to each control variable in the second step. The algorithm shown here has been implemented on various types of multiple instruction, multiple data parallel computers to simulate maximum-height jumping and walking. CPU, central processing unit. (Modified from Reference 38.)

the increase in computational time associated with the parameter optimization approach (92, 95). In particular, calculation of the derivatives of the cost function and the constraints with respect to the controls can be very expensive because the number of forward integrations equals the number of controls for each iteration of the parameter optimization algorithm (92, 94).

## Dynamic Optimization Problems can be Parallelized

Fortunately, rapid advances in computer technology over the past decade have significantly reduced the computational time needed to solve dynamic optimization problems using the parameter optimization approach. Parallel computing, in particular, allows multiple processors to be used to perform the forward integrations needed to compute the derivatives of the cost function and the constraints during each iteration of the algorithm (see Figure 8). Computation of the derivatives can be distributed among the various processors of a parallel machine because the forward integrations are all independent of one another. Thus, a 23-dof, 54-muscle model of the body can be used to solve a dynamic optimization problem for jumping with just 23 h of central processing unit (CPU) on a 128-processor IBM SP-2 (38). Using the same model to simulate one cycle of gait takes roughly 1000 times longer [10,000 h of CPU are needed to converge to a solution for walking using a Cray T3E (23, 71)], but even formulating problems of this size was unthinkable 10 years ago. As computational speed continues to increase, so does the feasibility of combining dynamic optimization theory with very detailed models of the body to simulate such complex motor tasks as walking.

## Simulations of Movement Should be Visualized

One of the keys to a successful simulation is a good initial guess for the control variables (e.g. joint torques and muscle excitations). The initial guess should be chosen such that the simulated movement is at least qualitatively similar to what is observed experimentally. Very fast computer graphics workstations, such as a Silicon Graphics Onyx 2, can be used to visualize the simulated movement in real time. The single-processor speed of these machines allows forward integrations to be executed very quickly so that the control histories can be adjusted on line as the simulation proceeds (Figure 9).

## HOW MODELING AND EXPERIMENTATION CAN BE INTEGRATED TO STUDY MOVEMENT

Dynamic optimization theory is most powerful when the problem is formulated so that movement is synthesized from the beginning to the end of the task; that is, when the problem is formulated with no kinematic constraints so that the solution is driven mainly by the nature of the cost function (see Figure 10). This is the most appealing way to pose the optimization problem, but it is also the most difficult



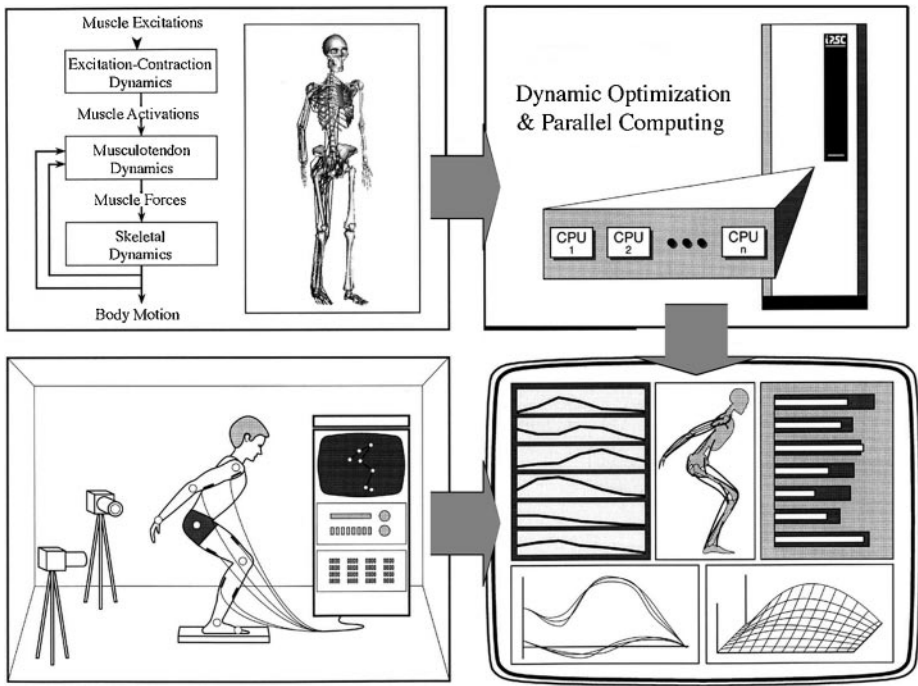


**Figure 10** Schematic diagram illustrating how musculoskeletal modeling (*top left*), dynamic optimization and high-performance computing (*top right*), in vivo experimentation (*bottom left*), and data analyses (*bottom right*) may be combined to study human movement. Here, the dynamic optimization problem is formulated and solved independent of experiment: Measurements of body motions, ground-reaction forces, and muscle activations are used only to evaluate the predictions of the model. Alternatively, modeling, dynamic optimization, and in vivo experimentation can be explicitly combined by formulating and solving a tracking problem (see text). CPU, central processing unit.

type of problem to solve. The reason is because the solution space remains very large when no constraints are used to bound it, and the time taken to converge to the optimal solution is then much longer. In a recent simulation of walking, the body-segmental motions, ground-reaction forces, muscle forces, and muscle excitation histories were predicted for one gait cycle given only the positions and velocities of the body segments at the beginning and end of the cycle (23, 71). The optimal solution was found by minimizing the total amount of metabolic energy consumed by the muscles per meter walked. Because the model was able to choose any movement pattern consistent with minimum metabolic cost, converging to the optimal solution took inordinately long [approximately 10,000 h of CPU (23, 71)].

Dynamic optimization problems may also be formulated so that the solution is constrained to follow a given path. For example, in the walking simulation

mentioned above, the joint angles and the components of the ground-reaction force may be treated as constraints that the solution must satisfy within a prescribed tolerance. The problem then is to find the muscle excitation histories (and muscle forces) that correspond to the measured patterns of body motions and ground forces. This approach, which has been used to simulate lower-limb (4, 8, 10, 45, 74) and upper-limb movements (96), is called tracking because the dynamic optimization solution is required to track a set of limb motion and external force measurements obtained from a motion analysis experiment (93). The method is appealing because by prescribing a path for the model to follow, the simulation is more likely to converge on a pattern of movement that is similar to what is observed in nature. Even when the trajectories of some of the dofs of the model cannot be measured accurately [e.g. tibiofemoral and tibioalcanal translations at the knee and ankle (97, 98)], the tracking approach can be used to constrain the model to follow those movements that can be measured and to predict all the remaining quantities (i.e. muscle forces and the translational movements of the bones at a joint) that cannot be measured. The main limitation of the tracking method is that it compromises the predictive power of the dynamic optimization approach; in particular, the tracking method cannot be used to predict how changes in body structure affect tissue function and task performance. On the other hand, its main advantages are that it improves the convergence characteristics of the dynamic optimization problem, and an optimal solution can generally be found with smaller investments of computer time.

## HOW SHOULD MODEL OUTPUT BE ANALYZED?

A muscle can contribute to the acceleration of a body segment without touching it. This conclusion follows from Equation 1, where the mass matrix,  $M(q)$ , has two important properties: (a) it is a function of the generalized coordinates,  $q$ , which specify the relative positions of the body segments; and (b) it is a nondiagonal matrix, meaning that its off-diagonal terms are always nonzero (82). These properties are preserved when  $M(q)$  is inverted, and so from Equation 3, all forces (i.e. Coriolis and centrifugal forces, gravity, muscle forces, and external forces) act to accelerate all body segments at each instant, thus

$$\ddot{q} = -M^{-1}(q)[C(q)\dot{q}^2 + G(q) + R(q)F^{MT} + E(q, \dot{q})], \quad (4)$$

where  $M^{-1}(q)$  denotes the inverse of the system mass matrix. Muscle's contribution to the accelerations of the body segments is then given by

$$\ddot{q}^{\text{mus}} = -M^{-1}(q)R(q)F^{MT}. \quad (5)$$

Equation 5 explains in mathematical terms why each muscle contributes to the acceleration of all the body segments. The physical explanation is as follows. When a muscle touches a body segment, it can apply a force to that segment; the force the muscle applies to that segment is transmitted up and down the multilink

chain via the contact forces acting at the joints. Thus, a muscle like soleus, which crosses only the ankle, can accelerate the tibia, the foot, and all the other segments in the body as well. The magnitudes of these induced accelerations depend on the relative positions of all the segments at the instant under consideration. In flat-footed posture, for example, when the knee is near full extension, a force developed in soleus can accelerate the knee further into extension twice as much as it acts to accelerate the ankle into extension. When the knee is bent to angles greater than  $90^\circ$ , however, a force developed in soleus acts to accelerate the knee into flexion (see Figure 6.12 in reference 82). Recent analyses have lead to similar conclusions about the function of soleus during pedaling as well (9) (see below). Body position affects the magnitude and direction of the acceleration of a body segment induced by a muscle force because it affects the torque applied by the muscle force to that segment. In the example above, soleus accelerates the knee into extension when the body is placed in a near-upright posture because the joint contact forces induced at the knee are oriented in such a way that they apply torques to the thigh and shank, which accelerate the knee into extension. When the knee is bent greater than  $90^\circ$ , however, the joint-reaction forces induced by soleus at the knee are oriented such that they then apply torques to the thigh and shank, which accelerate the knee into flexion.

## MODEL SIMULATIONS CAN REVEAL FUNCTION

Because the dynamic optimization approach produces the time histories of muscle forces, Equation 5 can be used to determine how muscles accelerate and generate power to the body segments during movement (6, 82). Muscle-induced accelerations have been used to study coordination of multijoint movement during various motor tasks, including standing (7), vertical jumping (99), walking (23, 28, 99a), and pedaling (8–10). In this section, I review some of the results obtained for vertical jumping and pedaling and present some recent findings for walking as well.

Jumping and pedaling are both well suited to the dynamic optimization approach. One uses both legs in unison to jump to one's maximum height; thus, two legs can be modeled as one, which simplifies the equations for skeletal dynamics (5). Jumping also presents a well-defined goal (i.e. to jump as high as possible). Pedaling, on the other hand, is performed seated, so balancing the upper body is not an issue (8, 9, 64). Also, because the crank is propelled through a constrained path, the muscles have fewer dofs to control.

### Jumping

Simulations of jumping have shown that muscles dominate the vertical acceleration of, and the power generated to, the body segments during propulsion; gravitational and inertial forces do not contribute much, except near liftoff, when the ankle, knee, and hip are all then rotating very quickly (99). The uniarticular gluteus maximus

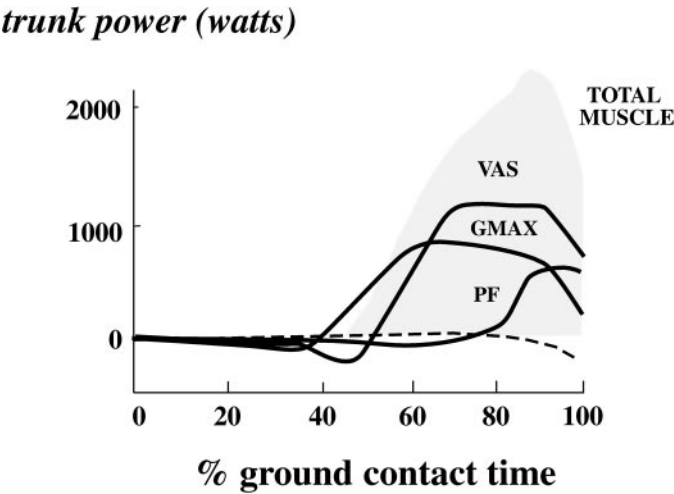


**Figure 11** Contributions of individual muscle groups to the total power generated to the trunk (head, arms, and torso) by all the leg muscles during the propulsion phase of a maximum-height jump. The area under the shaded curve represents the total energy generated to the trunk by all the muscles (TOTAL MUSCLE). Energy generated to the trunk by vasti (VAS), gluteus maximus (GMAX), and the ankle plantarflexors (PF) is represented by the area under each of these curves. PF represents the contribution from soleus and gastrocnemius in the model. The dashed line represents the contribution of all the other muscles in the model. These results were obtained by solving a dynamic optimization problem for jumping using a 4-segment, 4-dof, 8-muscle model of the body. The problem was to find the set of muscle excitations that produced the highest possible jump. (Modified from Reference 99.)

and vasti account for a large fraction of the total propulsive energy made available by all the muscles; these muscles also contribute 70% of the total power generated to the trunk (Figure 11). The biarticular muscles, especially rectus femoris and hamstrings, contribute little to liftoff velocity and, therefore, to jump height (32, 99).

Jumping to one's maximum height requires precise coordination of the actions of the gluteus maximus, vasti, and plantarflexors (including gastrocnemius). The sequence of muscle activity is proximal-to-distal (5, 33). Gluteus maximus works synergistically with vasti, whereas soleus and gastrocnemius function independently to accelerate the trunk upward. Both gluteus maximus and vasti accelerate the hip and the knee into extension, even though each muscle crosses only one of these joints. Hip and knee extension are needed to move the trunk upward during early propulsion, and not surprisingly, these tasks are performed by the two strongest muscles in the body. Soleus and gastrocnemius are activated just prior to liftoff, generating maximum power to the trunk at a time when neither gluteus

maximus nor vasti can sustain adequate levels of muscle force (because the hip and knee are near full extension at liftoff) (30, 99).

## Pedaling

Model simulations have shown that muscles dominate acceleration of the crank throughout the pedaling cycle; gravitational and inertial forces do not contribute much (8). As with jumping, gluteus maximus and vasti are the prime movers of the leg, providing more than half the energy needed for propulsion. In contrast to jumping, however, the biarticular muscles, particularly hamstrings and rectus femoris, appear to have well-defined roles in pedaling. These muscles make smooth pedaling possible by accelerating the crank through the stroke transitions (i.e. the transitions between top dead center and bottom dead center) (9, 10). One unanticipated result is that hamstrings act to accelerate the knee into extension in late downstroke. The extensor torque produced by hamstrings at the hip in late downstroke is greater than the flexor torque that this muscle produces at the knee. In addition, limb position at this time is such that a hip extensor torque is more readily able to accelerate the knee into extension than a knee flexor torque is able to accelerate the knee into flexion. Consequently, even though hamstrings produce a flexor torque at the knee, the net action is to assist in knee hyperextension during late downstroke. The knee does not hyperextend, however, because soleus acts to accelerate the knee into flexion at this time (see 9; Figure 6).

Are muscle synergies evident in pedaling? The answer appears to be yes. Six biomechanical functions have been identified and organized into three antagonistic pairs: upward-downward and anterior-posterior acceleration of the foot relative to the pelvis and upward-downward acceleration of the foot relative to the shank (100). Muscles work synergistically within the framework of this scheme to produce the most effective crank acceleration over each cycle. For example, soleus works synergistically with gluteus maximus and vasti by transferring energy from these muscles to the crank, where it is most needed for propulsion (10).

## Walking

Hundreds of papers have been written on walking; yet, we still have only a superficial understanding of how muscles work together to coordinate movement of the body parts during gait (2, 101). For normal walking, the leg muscles are called on to support the body against the downward force of gravity as well as to maintain forward progression at a more-or-less steady rate. Analysis of a dynamic optimization solution for normal gait has shown that gluteus maximus, gluteus medius, iliopsoas, vasti, soleus, and gastrocnemius are the prime movers, contributing up to 70% of the total mechanical energy produced by all the muscles (MG Pandy & FC Anderson, unpublished results). Gluteus maximus and vasti provide support against gravity during initial stance, gluteus medius during midstance, and soleus and gastrocnemius during terminal stance (Figure 12).

The muscles that contribute most in the fore-aft direction are soleus, vasti, and gastrocnemius. Vasti and soleus decelerate the body's center of mass (i.e. provide a backward acceleration) during the first half of stance, but then soleus and gastrocnemius propel the body forward during terminal stance and the first part of the ensuing double support phase (102) (Figure 12). Calculations of muscle-induced accelerations and power can also be used to more fully explain muscle synergies thought to be present during walking; for example, the gait simulation mentioned above could also be used to evaluate the hypothesis that vasti acts during midstance to accelerate the ankle into extension by retarding forward rotation of the shank, thereby helping soleus and gastrocnemius to prepare for push off during terminal stance (2, 103).

## LOOKING AHEAD

This is an exciting time for computational modeling in general and its application to the study of human movement in particular. With the birth of parallel computers and high-end graphics workstations, models of increasing complexity can be used to perform more realistic simulations of walking, running, throwing, etc. Although the entertainment industry may be interested in more detailed simulations of movement purely for the sake of increased realism (104), more advanced models and simulations are also needed to address some of the more pressing problems in orthopedics and sports medicine. For example, detailed models of body structure are needed not only to describe muscle function during normal gait, but also to evaluate surgical procedures designed to correct abnormalities seen in the gait patterns of cerebral palsy and stroke victims. Detailed models are also needed to more fully describe and explain the interactions between muscles, ligaments, and bones in intact, injured, and reconstructed joints. At the knee, for example, more accurate representations of muscle, tendon, ligament, and bone structure will enable modeling to be used to study how joint function is affected by procedures, such as anterior cruciate ligament (ACL) reconstructions and high tibial osteotomies (105, 106).

Increasing computer speed will also enable models of greater complexity to be used to study mechanics and energetics at a much deeper level than has been possible to date. The model shown in Figure 3 has been used together with dynamic optimization theory to describe how muscles coordinate motion of the body segments during normal walking (23). If the time taken to converge to a solution could be decreased by formulating and solving a tracking problem (see above), then this model could also be used to study how muscle function changes when walking speed, incline of the ground, and body structure change independently. Because the dynamic optimization solution gives detailed information about the forces developed by the leg muscles for each perturbation introduced to the model, analyses of the simulation results will allow rigorous testing of the hypothesis that metabolic cost of movement is determined mainly by the cost of generating muscle force (107, 108).

Certainly one of the most significant challenges facing the modeling community today is finding new ways to more accurately describe structure of the musculoskeletal system (e.g. moment arms, muscle-fiber and tendon rest lengths, muscle cross-sectional areas, and muscle pennation angles). There is some evidence to suggest that musculoskeletal geometry (i.e. muscle paths) is the most critical element of the modeling process described in Figure 2 (109, 110). In gait studies, for example, calculated values of muscle force depend more heavily on estimates of muscle moment arms than on the mechanical properties of the muscles themselves (42, 88, 110). This finding is one of the reasons why generic models are sometimes criticized (111), and it is also the impetus for using techniques such as computed tomography and magnetic resonance imaging to model body structure more accurately (112–114). Unfortunately, application of these techniques is still an expensive proposition, so much so that cost is often named as the major factor limiting the use of subject-specific models in gait analysis and surgery simulation.

Even if computed tomography and magnetic resonance imaging could be used cost-effectively to develop subject-specific models of musculoskeletal geometry, there are bound to be instances, most likely in movements such as running, jumping, and throwing, which are performed at higher frequencies, where the activation and contractile properties of muscle play a significant role in determining the development of muscle force. Take vertical jumping, for example, where model simulation results indicate that performance is strongly dependent on the values assumed for muscle cross-sectional area, muscle-fiber contraction speed, and the rise and relaxation times for muscle activation (60, 89, 90). If tasks such as this are to be studied in even greater detail, then better estimates will be needed on a muscle-by-muscle basis for the intrinsic maximum shortening velocity of muscle and for activation rise and relaxation times. Determining the values of muscle-specific parameters is even more daunting when pathology is present. For example, spasticity caused by stroke and cerebral palsy may alter the force-length and force-velocity properties of muscle (115), but how can these effects be monitored *in vivo*, and how should tissue adaptation that accompanies pathology and immobilization after surgery be represented in a computer model of the body? More research is needed to learn how best to obtain *in vivo* estimates of the geometry and properties of the neuromusculoskeletal system so that these data may be integrated into the subject-specific modeling process.

## ACKNOWLEDGMENTS

Frank C Anderson performed the muscle-induced-acceleration analysis reported for normal walking. It is a pleasure also to acknowledge Patty Coffman's help with figure preparation. Various portions of the work reported here were supported in part by the Whitaker Foundation and NASA. Computational support was provided by the Center for High Performance Computing and the Visualization Lab at the University of Texas at Austin.

Visit the Annual Reviews home page at [www.AnnualReviews.org](http://www.AnnualReviews.org)

## LITERATURE CITED

1. Winter DA. 1990. *Biomechanics and Motor Control of Human Movement*. New York: Wiley
2. Perry J. 1992. *Gait Analysis: Normal and Pathological Function*. Thorofare, NJ: SLACK
3. Vaughan CL, Davis BL, O'Connor J. 1992. *Dynamics of Human Gait*. Champaign, IL: Hum. Kinet.
4. Yamaguchi GT, Zajac FE. 1990. Restoring unassisted natural gait to paraplegics via functional neuromuscular stimulation: a computer simulation study. *IEEE Trans. Biomed. Eng.* 37:886–902
5. Pandy MG, Zajac FE, Sim E, Levine WS. 1990. An optimal control model for maximum-height human jumping. *J. Biomech.* 23:1185–98
6. Zajac FE. 1993. Muscle coordination: a perspective. *J. Biomech.* 26(Suppl. 1): 109–24
7. Kuo AD, Zajac FE. 1993. A biomechanical analysis of muscle strength as a limiting factor in standing posture. *J. Biomech.* 26(Suppl. 1):137–50
8. Fregly BJ, Zajac FE. 1996. A state-space analysis of mechanical energy generation, absorption, and transfer during pedaling. *J. Biomech.* 29:81–90
9. Raasch CC, Zajac FE, Ma B, Levine WS. 1997. Muscle coordination of maximum-speed pedaling. *J. Biomech.* 6:595–602
10. Neptune RR, Kautz SA, Zajac FE. 2000. Muscle contributions to specific biomechanical functions do not change in forward versus backward pedaling. *J. Biomech.* 33:155–64
11. Cavagna GA, Heglund NC, Taylor RC. 1977. Mechanical work in terrestrial locomotion: two basic mechanisms for minimizing energy expenditure. *Am. J. Physiol.* 233:R243–61
12. McMahon TA. 1984. *Muscles, Reflexes, and Locomotion*. Princeton, NJ: Princeton Univ. Press
13. Farley CT, Ferris DP. 1998. Biomechanics of walking and running: center of mass movements to muscle action. *Exerc. Sport Sci. Rev.* 26:253–85
14. Mochon S, McMahon TA. 1980. Ballistic walking. *J. Biomech.* 13:49–57
15. Mena D, Mansour JM, Simon SR. 1981. Analysis and synthesis of human swing leg motion during gait and its clinical applications. *J. Biomech.* 14:823–32
16. Pandy MG, Berme N. 1988. Synthesis of human walking: a planar model for single support. *J. Biomech.* 21:1053–60
17. Gilchrist LA, Winter DA. 1997. A multi-segment computer simulation of normal human gait. *IEEE Trans. Rehabil. Eng.* 5:290–99
18. Yoon YS, Mansour JM. 1982. The passive elastic moment at the hip. *J. Biomech.* 15:905–10
19. Mansour JM, Audu ML. 1986. The passive elastic moment at the knee and its influence on human gait. *J. Biomech.* 19:369–73
20. Engin AE. 1980. On the biomechanics of the shoulder complex. *J. Biomech.* 13:575–90
21. Audu ML. 1987. *Optimal control modeling of lower extremity musculoskeletal motion*. PhD thesis. Case Western Reserve Univ., Cleveland, OH. 216 pp.
22. Hatze H. 1997. A three-dimensional multivariate model of passive human joint torques and articular boundaries. *Clin. Biomech.* 12:128–35
23. Anderson FC. 1999. *A dynamic optimization solution for a complete cycle of normal gait*. PhD thesis. Univ. Tex., Austin. 440 pp.
24. Shrive NG, O'Connor JJ, Goodfellow



- JW. 1978. Load-bearing in the knee joint. *Clin. Orthop. Relat. Res.* 131:279–87
25. Kuo AD. 1995. An optimal control model for analyzing human postural balance. *IEEE Trans. Biomed. Eng.* 42:87–101
  26. Pandy MG, Berme N. 1988. A numerical method for simulating the dynamics of human walking. *J. Biomech.* 21:1043–51
  27. Taga G. 1995. A model of the neuromusculoskeletal system for human locomotion: emergence of basic gait. *Biol. Cybernet.* 73:95–111
  28. Piazza SJ, Delp SL. 1996. The influence of muscles on knee flexion during the swing phase of gait. *J. Biomech.* 29:723–33
  29. Cole GK, Nigg BM, van den Bogert AJ. 1996. Lower extremity joint loading during impact in running. *Clin. Biomech.* 11:181–93
  30. Anderson FC, Pandy MG. 1993. Storage and utilization of elastic strain energy during jumping. *J. Biomech.* 26:1413–27
  31. Selbie WS, Caldwell GE. 1996. A simulation study of vertical jumping from different starting postures. *J. Biomech.* 29:1137–46
  32. van Soest AJ, Schwab AL, Bobbert MF, van Ingen Schenau GJ. 1993. The influence of the biarticularity of the gastrocnemius muscle on vertical-jumping performance. *J. Biomech.* 26:1–8
  33. Bobbert MF, van Ingen Schenau GJ. 1988. Coordination in vertical jumping. *J. Biomech.* 21:249–62
  34. Saunders JB, Inman VT, Eberhart HD. 1953. The major determinants in normal and pathological gait. *J. Bone Joint Surg.* 35A:543–58
  35. Onyshko S, Winter DA. 1980. A mathematical model for the dynamics of human locomotion. *J. Biomech.* 13:361–68
  36. Ju MS, Mansour JM. 1988. Simulation of the double limb support phase of human gait. *J. Biomech. Eng.* 110:223–29
  37. Gerritsen KGM, van den Bogert AJ, Nigg BM. 1995. Direct dynamics simulation of the impact phase in heel-toe running. *J. Biomech.* 28:661–68
  38. Anderson FC, Pandy MG. 1999. A dynamic optimization solution for vertical jumping in three dimensions. *Comput. Methods Biomech. Biomed. Eng.* 2:201–31
  39. Morrison JB. 1970. The mechanics of the knee joint in relation to normal walking. *J. Biomech.* 3:51–61
  40. Seireg A, Arvikar RJ. 1973. A mathematical model for evaluation of forces in the lower extremities of the musculoskeletal system. *J. Biomech.* 6:313–26
  41. Hardt DE. 1978. Determining muscle forces in the leg during human walking: an application and evaluation of optimization methods. *J. Biomech. Eng.* 100:72–78
  42. Patriarco AB, Mann RW, Simon SR, Mansour JM. 1981. An evaluation of the approaches of optimization methods in the prediction of muscle forces during human gait. *J. Biomech.* 14:513–25
  43. Hatze H. 1976. The complete optimization of human motion. *Math. Biosci.* 28:99–35
  44. Crowninshield RD, Brand RA. 1981. A physiologically based criterion of muscle force prediction in locomotion. *J. Biomech.* 14:793–801
  45. Davy DT, Audu ML. 1987. A dynamic optimization technique for predicting muscle forces in the swing phase of gait. *J. Biomech.* 20:187–201
  46. Hoy MG, Zajac FE, Gordon ME. 1990. A musculoskeletal model of the human lower extremity: the effect of muscle, tendon, and moment arm on the moment-angle relationship of musculotendon actuators at the hip, knee, and ankle. *J. Biomech.* 23:157–69
  47. Jensen RH, Davy DT. 1975. An investigation of muscle lines of action about the hip: a centroid line approach vs the straight line approach. *J. Biomech.* 8:103–10
  48. Pierrynowski MR. 1995. Analytic representation of muscle line of action and

- geometry. In *Three-Dimensional Analysis of Human Movement*, ed. P Allard, IAF Stokes, JP Blanchi, pp. 214–56. Champaign, IL: Hum. Kinet.
49. Seireg A, Arvikar RJ. 1989. *Biomechanical Analysis of the Musculoskeletal Structure for Medicine and Sports*. New York: Hemisphere
  50. Brand RA, Crowninshield RD, Wittstock CE, Pedersen DR, Clark CR, van Krieken FM. 1982. A model of lower extremity muscular anatomy. *J. Biomech. Eng.* 104:304–10
  51. Delp SL, Loan JP, Hoy MG, Zajac FE, Topp EL, Rosen JM. 1990. An interactive graphics-based model of the lower extremity to study orthopaedic surgical procedures. *IEEE Trans. Biomed. Eng.* 37:757–67
  52. Hogfors C, Sigholm G, Herberts P. 1987. Biomechanical model of the human shoulder. I. Elements. *J. Biomech.* 20:157–66
  53. van der Helm FC, Veeger HE, Pronk GM, van der Woude LH, Rozendal RH. 1992. Geometry parameters for musculoskeletal modeling of the shoulder system. *J. Biomech.* 25:129–44
  54. Garner BA. 1998. *A musculoskeletal model of the upper limb based on the medical image dataset of the Visible Human Male*. PhD thesis. Univ. Tex., Austin. 295 pp.
  55. Garner BA, Pandy MG. 2000. The obstacle-set method for representing muscle paths in musculoskeletal models. *Comput. Methods Biomech. Biomed. Eng.* 3:1–30
  56. Winters JM, Stark L. 1985. Analysis of fundamental human movement patterns through the use of in-depth antagonistic muscle models. *IEEE Trans. Biomed. Eng.* BME-32:826–39
  57. Zajac FE. 1989. Muscle and tendon: properties, models, scaling, and application to biomechanics and motor control. *CRC Crit. Rev. Biomed. Eng.* 19:359–411
  58. Yamaguchi GT, Sawa AGU, Moran DW, Fessler MJ, Winters JM. 1990. A survey of human musculotendon actuator parameters. See Ref. 116, pp. 717–51
  59. Klein-Breteler MD, Spoor CW, van der Helm FCT. 1999. Measuring muscle and joint geometry parameters of a shoulder for modeling purposes. *J. Biomech.* 32:1191–97
  60. Pandy MG. 1990. An analytical framework for quantifying muscular action during human movement. See Ref. 116, pp. 653–62
  61. Butler DL, Grood ES, Noyes FR, Zernicke RF. 1979. Biomechanics of ligaments and tendons. *Exerc. Sport Sci. Rev.* 6:125–81
  62. Woo SL-Y. 1982. Mechanical properties of tendons and ligaments. I. Quasi-static and nonlinear coelastic properties. *Biorheology* 19:385–96
  63. Ebashi S, Endo M. 1968. Calcium ion and muscle contraction. *Progr. Biophys. Mol. Biol.* 18:125–83
  64. Schutte LM, Rodgers MM, Zajac FE. 1993. Improving the efficacy of electrical stimulation-induced leg cycle ergometry: an analysis based on a dynamic musculoskeletal model. *IEEE Trans. Rehabil. Eng.* 1:109–25
  65. Hatze H. 1978. A general myocybernetic control model of skeletal muscle. *Biol. Cybernet.* 28:143–57
  66. Happee R. 1994. Inverse dynamic optimization including muscular dynamics, a new simulation method applied to goal directed movements. *J. Biomech.* 27:953–60
  67. Deleted in proof
  68. Hof AL, Pronk CAN, van Best JA. 1987. Comparison between EMG to force processing and kinetic analysis for the calf muscle moment in walking and stepping. *J. Biomech.* 20:167–78
  69. White SC, Winter DA. 1993. Predicting muscle forces in gait from EMG signals and musculotendon kinematics. *J. Electromyogr. Kinesiol.* 2:217–31
  70. Pandy MG, Garner BA, Anderson FC. 1995. Optimal control of non-ballistic

- muscular movements: a constraint-based performance criterion for rising from a chair. *J. Biomech. Eng.* 117:15–26
71. Anderson FC, Pandy MG. 2001. Dynamic optimization of human walking. *J. Biomech. Eng.* In press
  72. Ralston HJ. 1958. Energetics of human walking. In *Neural Control of Locomotion*, ed. RM Herman, S Grillner, P Stein, DG Stuart, pp. 77–98. New York: Plenum
  73. Marshall RN, Wood GA, Jennings LS. 1989. Performance objectives in human movement: a review and application to the stance phase of normal walking. *Hum. Move. Sci.* 8:571–94
  74. Neptune RR, Kautz SA, Hull ML. 1998. Evaluation of performance criteria for simulation of submaximal steady-state cycling using a forward dynamic model. *J. Biomech. Eng.* 120:334–41
  75. Collins JJ. 1996. The redundant nature of locomotor optimization laws. *J. Biomech.* 28:251–67
  76. Hubbard M, Alaways LW. 1989. Rapid and accurate estimation of release conditions in the javelin throw. *J. Biomech.* 22:583–95
  77. Pandy MG, Anderson FC. 2000. Dynamic simulation of human movement using large-scale models of the body. *Phonetica* 57:219–28
  78. Komi PV. 1990. Relevance of in vivo force measurements to human biomechanics. *J. Biomech.* 23:23–43
  79. Gregor RJ, Abelew TA. 1994. Tendon force measurements and movement control: a review. *Med. Sci. Sports Exerc.* 26:1359–72
  80. Glitsch U, Baumann W. 1997. The three-dimensional determination of internal loads in the lower extremity. *J. Biomech.* 30:1123–31
  81. Shelburne KB, Pandy MG. 1997. A musculoskeletal model of the knee for evaluating ligament forces during isometric contractions. *J. Biomech.* 30:163–76
  82. Zajac FE, Gordon ME. 1989. Determining muscle's force and action in multi-articular movement. *Exerc. Sport Sci. Rev.* 17:187–230
  83. Pierrynowski M, Morrison JB. 1985. A physiological model for the evaluation of muscular forces in human locomotion: theoretical aspects. *Math. Biosci.* 75:69–101
  84. Sepulveda F, Wells DM, Vaughan CL. 1993. A neural network representation of electromyography and joint dynamics in human gait. *J. Biomech.* 26:101–9
  85. Vaughan CL, Brookings GD, Olree KS. 1996. Exploring new strategies for controlling multiple muscles in human locomotion. In *Human Motion Analysis: Current Applications and Future Directions*, ed. GF Harris, PA Smith, pp. 93–113. New York: IEEE
  86. Winter DA, Sidwall G, Hobson DA. 1974. Measurement and reduction of noise in kinematics of locomotion. *J. Biomech.* 7:157–59
  87. Ladin Z, Flowers WC, Messner W. 1989. A quantitative comparison of a position measurement system and accelerometry. *J. Biomech.* 22:295–308
  88. Anderson FC, Pandy MG. 2001. Static and dynamic optimization solutions for gait are practically equivalent. *J. Biomech.* 34:153–61
  89. Zajac FE, Wicke RW, Levine WS. 1984. Dependence of jumping performance on muscle properties when humans use only calf muscles for propulsion. *J. Biomech.* 17:513–23
  90. van Soest AJ, Bobbert MF. 1993. The contribution of muscle properties in the control of explosive movements. *Biol. Cybernet.* 69:195–204
  91. Chow CK, Jacobson DH. 1971. Studies of human locomotion via optimal programming. *Math. Biosci.* 10:239–306
  92. Anderson FC, Ziegler JM, Pandy MG, Whalen RT. 1995. Application of high-performance computing to numerical simulation of human movement. *J. Biomech. Eng.* 117:155–57
  93. Bryson AE, Ho YC. 1975. *Applied*

- Optimal Control*. Washington, DC: Hemisphere
94. Pandy MG, Anderson FC, Hull DG. 1992. A parameter optimization approach for the optimal control of large-scale musculoskeletal systems. *J. Biomech. Eng.* 114:450–60
  95. Neptune RR. 1999. Optimal algorithm performance in determining optimal controls in human movement analysis. *J. Biomech. Eng.* 121:249–52
  96. Hannaford B, Kim WS, Lee SH, Stark L. 1986. Neurological control of head movements: inverse modeling and electromyographic evidence. *Math. Biosci.* 78:159–78
  97. LaFortune MA, Cavanagh PR, Sommer HJ, Kalenak A. 1992. Three-dimensional kinematics of the human knee during walking. *J. Biomech.* 25:347–57
  98. Stacoff A, Nigg BM, Reinschmidt C, van den Bogert AJ, Lundberg A. 2000. Tibio-calcaneal kinematics of barefoot versus shod running. *J. Biomech.* 33:1387–95
  99. Pandy MG, Zajac FE. 1991. Optimal muscular coordination strategies for jumping. *J. Biomech.* 24:1–10
  - 99a. Kepple TM, Seigel KL, Stanhope SJ. 1997. Relative contributions of the lower extremity joint moments to forward progression and support during gait. *Gait Posture* 6:1–8
  100. Ting LH, Kautz SA, Brown DA, Zajac FE. 1999. Phase reversal of biomechanical functions and muscle activity in backward pedaling. *J. Neurophysiol.* 81:544–51
  101. Rose J, Gamble JG. 1994. *Human Walking*. Baltimore, MD: Williams Wilkins
  102. Anderson FC, Pandy MG. 2001. Contributions of individual muscles to support during normal gait. *Gait Posture* 13:292–93
  103. Brandell BR. 1977. Functional roles of the calf and vastus muscles in locomotion. *Am. J. Phys. Med.* 56:59–74
  104. Hodgins J, Wooten W, Brogan D, O'Brien J. 1995. Animating human athletics. Computer graphics. *Proc. SIGGRAPH*, pp. 71–78.
  105. Loch DA, Luo Z, Lewis JL, Stewart NJ. 1991. A theoretical model of the knee and ACL: theory and experimental verification. *J. Biomech.* 25:81–90
  106. Chao EYS, Lynch JD, Vanderploeg MJ. 1993. Simulation and animation of musculoskeletal joint system. *J. Biomech. Eng.* 115:562–68
  107. Taylor CR, Heglund NC, McMahon TA, Looney TR. 1980. Energetic cost of generating muscular force during running: a comparison of large and small animals. *J. Exp. Biol.* 86:9–18
  108. Kram R, Taylor CR. 1990. Energetics of running: a new perspective. *Nature* 346:265–67
  109. Herzog W. 1992. Sensitivity of muscle force estimation to changes in muscle input parameters using nonlinear optimization. *J. Biomech. Eng.* 114:267–68
  110. Brand RA, Pedersen DR, Davy DT, Kotzar GM, Heiple KG, Goldberg VM. 1994. Comparison of hip force calculations and measurements in the same patient. *J. Arthroplasty* 9:45–51
  111. Blankevoort L, Huiskes R. 1996. Validation of a three-dimensional model of the knee. *J. Biomech.* 29:955–61
  112. Garner BA, Pandy MG. 2001. Musculoskeletal model of the upper limb based on the Visible Human Male dataset. *Comput. Methods Biomech. Biomed. Eng.* 4: In press
  113. Salinas S, Arnold A, Schmidt DJ, Delp SL. 1999. Accuracy of subject-specific musculoskeletal models derived from magnetic resonance images. *Proc. 7th Int. Symp. Comput. Simul. Biomech., Univ. Calgary, Calgary, Can.,* pp. 18–21. Canada: Univ. Calgary Publ.
  114. Cohen ZA, McCarthy DM, Roglic H, Henry JH, Rodkey WG, et al. 1998. Computer-aided planning of patellofemoral joint OA surgery: developing

- physical models from patient MRI. In *Lecture Notes in Computer Science 1496*, ed. WM Wells, A Colchester, SL Delp, pp. 9–20. Berlin: Springer-Verlag
115. Slager UT, Hsu JD, Jordon C. 1985. Histochemical and morphological changes in muscles of stroke patients. *Clin. Orthop. Relat. Res.* 199:159–68
116. Winters JM, Woo SL-Y, eds. 1990. *Multiple Muscle Systems: Biomechanics and Movement Organization*. New York: Springer-Verlag

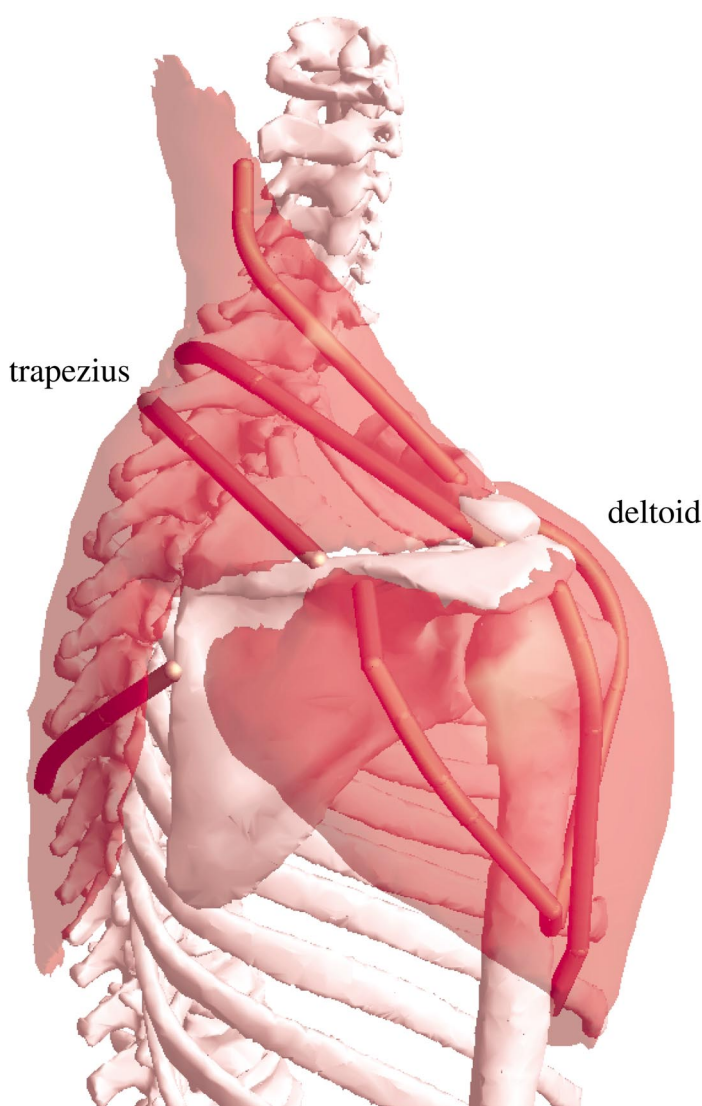


**Figure 4** Computer-generated rendering of the fan-shaped trapezius and deltoid muscles included in a model of the shoulder. Multiple paths were used to model the action of each muscle group. In this model, the trapezius was separated into four bundles and the deltoid into three. The geometry of the bones and the centroid paths of the muscles were based on three-dimensional reconstructions of high-resolution medical images obtained from the National Library of Medicine's Visible Human Male dataset. The muscle attachment sites were found by computing the centroids of the sets of triangles that defined the attachment sites of the muscles on the reconstructed surfaces of the bones (54, 112).

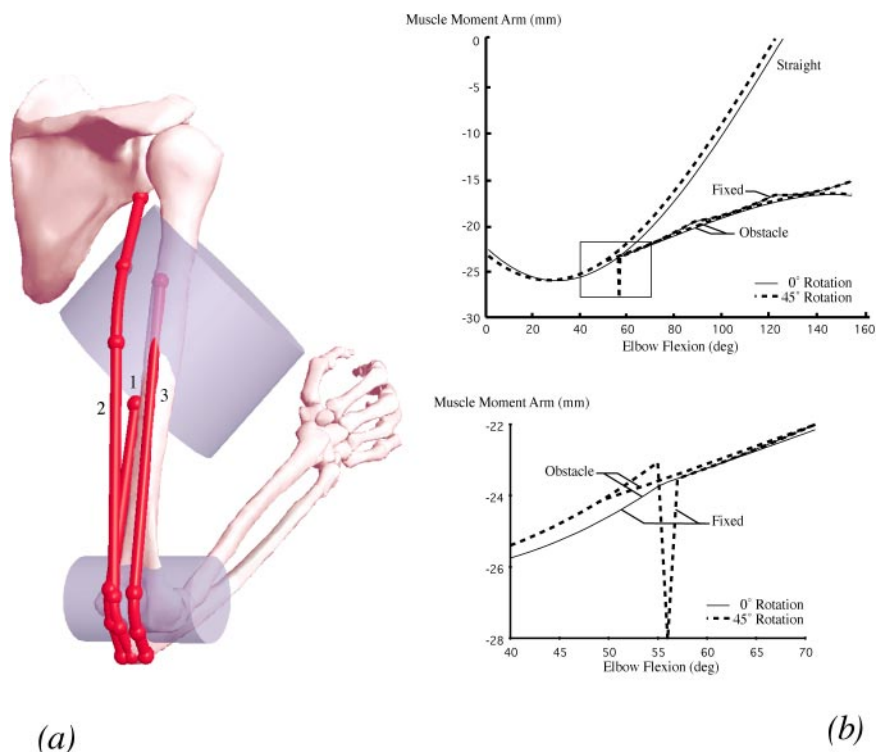


**Figure 5** (a) Posterolateral view of the obstacle-set model used to represent the paths of the three heads of triceps brachii in a model of the arm. The medial (1) and lateral head (3) were each modeled using a single-cylinder obstacle set (not shown). The long head (2) was modeled using a double-cylinder obstacle set, as illustrated here. The locations of the attachment sites of the muscle and the locations and orientations of the obstacles were chosen to reproduce the centroid paths of each portion of the modeled muscle. The geometry of the bones and the centroid paths of the muscles were based on three-dimensional reconstructions of high-resolution medical images obtained from the National Library of Medicine's Visible Human Male dataset. (b) Comparison of moment arms (*top*) for the long head of triceps obtained using the straight-line model (Straight), fixed-via-point model (Fixed), and the obstacle-set model (Obstacle). For each model, the moment arms were calculated over the full range of elbow flexion, with the humerus positioned alongside the torso in neutral rotation (solid lines) and in 45° internal rotation (dotted lines). (*Bottom*) Expanded scale of the graph above, where the moment arms obtained using the fixed-via-point and obstacle-set models are shown near the elbow flexion angle where the muscle first begins to wrap around the obstacle (cylinder) placed at the elbow (see A). The Fixed model produces a discontinuity in moment arm when the shoulder is rotated 45° internally (dotted line). (Modified from Reference 55.)

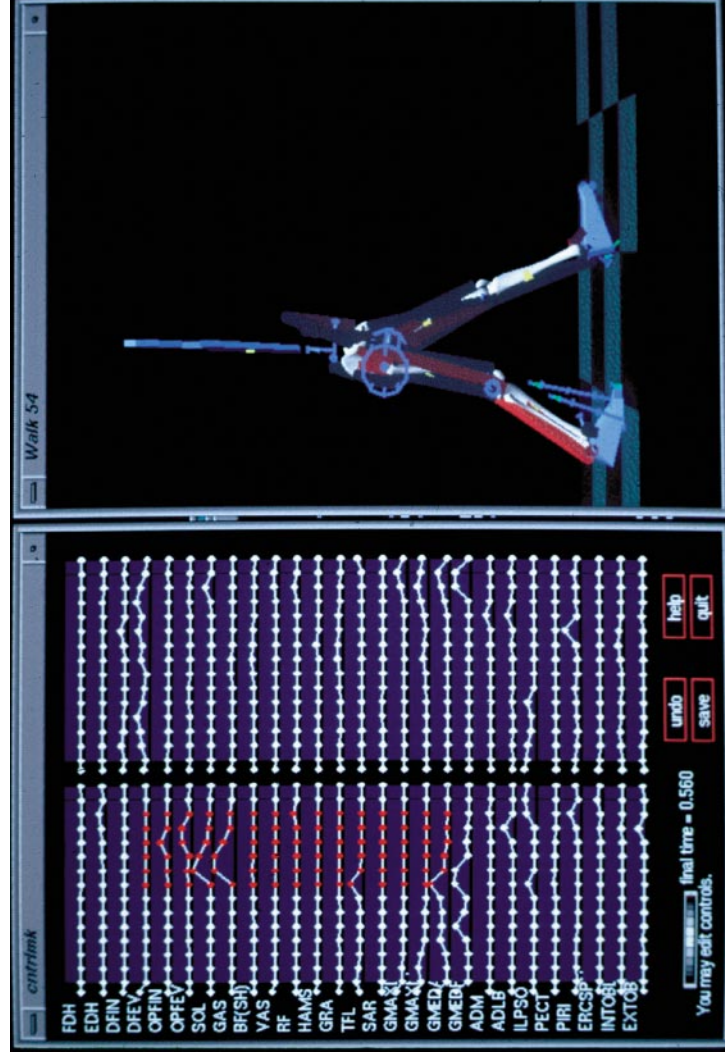


**Figure 9** Computer image showing a snapshot of a walking simulation performed using the 10-segment, 23-dof model shown in Figure 3. (*Left*) The muscle excitation signals input to the model during the simulation. The muscle excitations were found by solving a dynamic optimization problem that minimized the amount of metabolic energy consumed by all the muscles in the model per meter walked. The problem was solved using the computational algorithm shown in Figure 8. The simulation was visualized on a Silicon Graphics multiprocessor Onyx workstation.



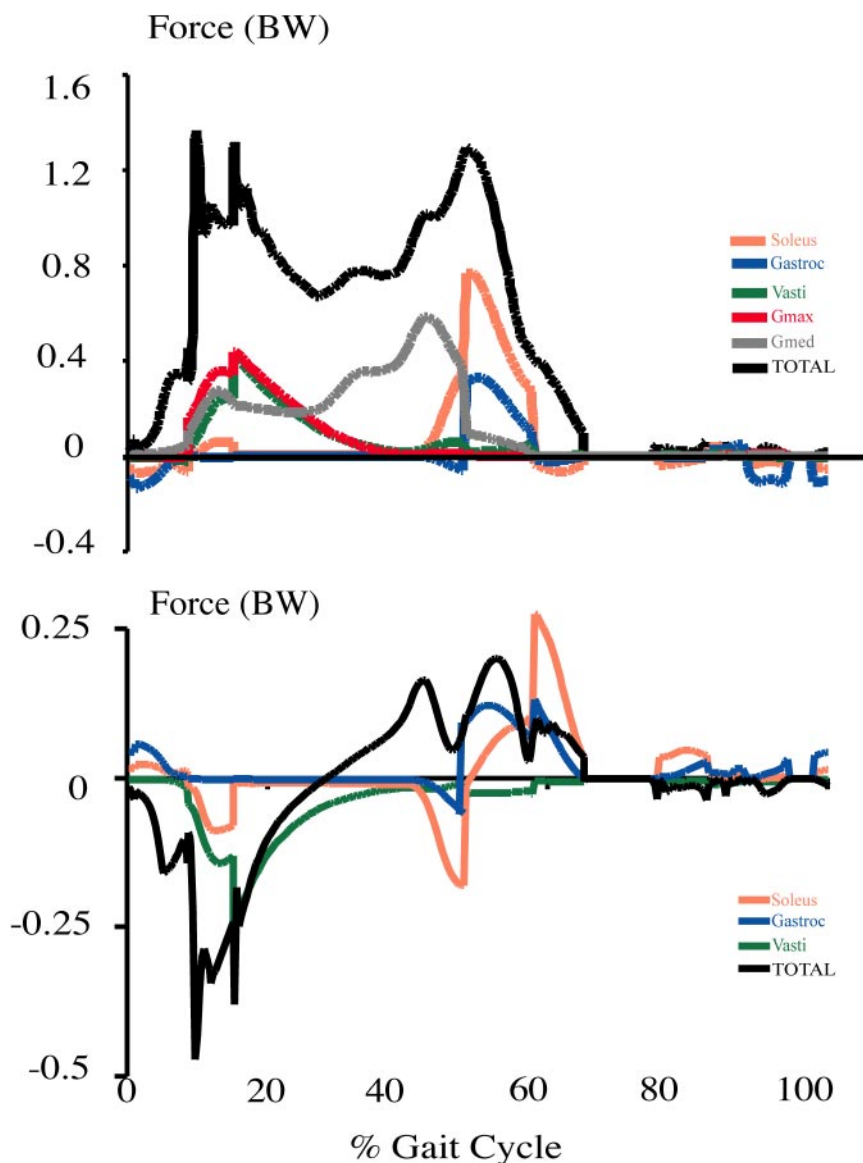


**Figure 12** Contributions of individual muscles to support (*top*) and progression (*bottom*) during gait. The results were obtained by solving a dynamic optimization problem for one cycle of normal walking using a 10-segment, 23-dof, 54-muscle model of the body (23, 71) (see Figure 3). Each muscle's contribution to support is given by its contribution to the vertical force exerted on the ground. Similarly, each muscle's contribution to progression is defined by its contribution to the fore-aft component of the ground-reaction force vector. BW, body weight.



## CONTENTS

---

THOMAS MCMAHON: A DEDICATION IN MEMORIAM, <i>Robert D. Howe and Richard E. Kronauer</i>	i
BIOMECHANICS OF CARDIOVASCULAR DEVELOPMENT, <i>Larry A. Taber</i>	1
FUNDAMENTALS OF IMPACT BIOMECHANICS: PART 2—BIOMECHANICS OF THE ABDOMEN, PELVIS, AND LOWER EXTREMITIES, <i>Albert I. King</i>	27
CARDIAC ENERGY METABOLISM: MODELS OF CELLULAR RESPIRATION, <i>M. Saleet Jafri, Stephen J. Dudycha, and Brian O'Rourke</i>	57
THE PROCESS AND DEVELOPMENT OF IMAGE-GUIDED PROCEDURES, <i>Robert L. Galloway, Jr.</i>	83
CAN WE MODEL NITRIC OXIDE BIOTRANSPORT? A SURVEY OF MATHEMATICAL MODELS FOR A SIMPLE DIATOMIC MOLECULE WITH SURPRISINGLY COMPLEX BIOLOGICAL ACTIVITIES, <i>Donald G. Buerk</i>	109
VISUAL PROSTHESES, <i>Edwin M. Maynard</i>	145
MICRO- AND NANOMECHANICS OF THE COCHLEAR OUTER HAIR CELL, <i>W. E. Brownell, A. A. Spector, R. M. Raphael, and A. S. Popel</i>	169
NEW DNA SEQUENCING METHODS, <i>Andre Marziali and Mark Akeson</i>	195
VASCULAR TISSUE ENGINEERING, <i>Robert M. Nerem and Dror Seliktar</i>	225
COMPUTER MODELING AND SIMULATION OF HUMAN MOVEMENT, <i>Marcus G. Pandy</i>	245
STEM CELL BIOENGINEERING, <i>Peter W. Zandstra and Andras Nagy</i>	275
BIOMECHANICS OF TRABECULAR BONE, <i>Tony M. Keaveny, Elise F. Morgan, Glen L. Niebur, and Oscar C. Yeh</i>	307
SOFT LITHOGRAPHY IN BIOLOGY AND BIOCHEMISTRY, <i>George M. Whitesides, Emanuele Ostuni, Shuichi Takayama, Xingyu Jiang, and Donald E. Ingber</i>	335
IMAGE-GUIDED ACOUSTIC THERAPY, <i>Shahram Vaezy, Marilee Andrew, Peter Kaczowski, and Lawrence Crum</i>	375
CONTROL MOTIFS FOR INTRACELLULAR REGULATORY NETWORKS, <i>Christopher V. Rao and Adam P. Arkin</i>	391

RESPIRATORY FLUID MECHANICS AND TRANSPORT PROCESSES, <i>James B. Grothberg</i>	421
--	-----

## INDEXES

Subject Index	459
Cumulative Index of Contributing Authors, Volumes 1–3	481
Cumulative Index of Chapter Titles, Volumes 1–3	483

## ERRATA

An online log of corrections to *Annual Review of Biomedical Engineering* chapters (1997 to the present) may be found at <http://bioeng.AnnualReviews.org/errata.shtml>.